Electronic Supplementary Material (ESI) for Journal of Materials Chemistry A.
This journal is © The Royal Society of Chemistry 2020

Grain size control of crystalline III-V semiconductors at ambient conditions using electrochemically mediated growth

Marco Valenti,[a†] Yorick Bleiji,[a†] Javier Blanco Portals,[b] Loreta A. Muscarella,[a] Mark Aarts,[a] Francesca Peiro,[b] Sonia Estrade[b] and Esther Alarcón-Lladó[a*]

[a]*Center for Nanophotonics, NWO-I AMOLF, Science Park 104, 1098 XG Amsterdam, The Netherlands*
[b]*Universitat de Barcelona, Catalunya, Spain*

+ These authors contributed equally
* email: E.Alarconllado@amolf.nl

Supplementary information

S1. Electron backscatter diffraction (EBSD)

EBSD measurements were carried out to probe the grain size and the microstructure of the In foil substrate. EBSD is a SEM-based technique where the electron beam interacts with a sample tilted by 70° and back-scattered electrons are collected using a direct electron detector placed at few cm from the specimen. The settings used for the EBSD measurement are: 15 keV, 800 pA, 50 ms as voltage, current specimen and exposure time for each pixel, respectively. 3 μm was used as step size and the working distance used was 13 mm. The interaction between the back-scattered electrons and the flat screen of the detector produce diffraction patterns (Kikuchi patterns). The Hough space (obtained by the conversion of the Kikuchi lines into points) is fitted with a tetragonal structure (I4/mmm space group) to obtain information about the crystal orientation and the grain size of In. In Figure S1 we observe grains of 100-200 μm of different crystallographic orientations in agreement with the polycrystalline nature of the indium foil.

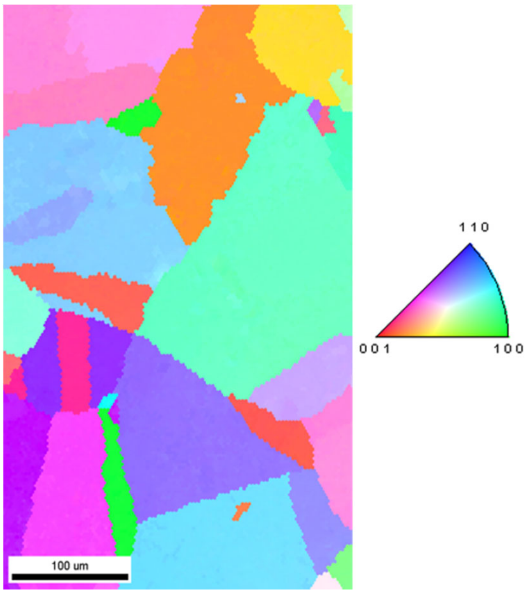

Figure S1. Inverse Pole Figure (IPF) map of Indium foil showing different crystallographic orientation along the z-direction (perpendicular to the substrate).

S2. Arsine generation

The reduction potential of an electrochemical reaction given by

$$aA + bB + n\,e^{-} \leftrightarrow C$$

is calculated using the Nernst equation,

$$E = E^{0} - \frac{k_B T}{n\;e} ln \frac{[C]}{[A]^{a}[B]^{b}}$$

where E^0 is the standard reduction potential, k_B is the Boltzmann constant, T is the temperature, n is the number of involved electrons, e is the elementary charge, $[x]$ are the concentrations.

In the case of hydrogen evolution, the reduction of As^{3+} ions, and arsine evolution we consider the following electrochemical reactions:

$2H^{+} + 2\,e^{-} \leftrightarrow\ H_2$, E^0=0 V vs SHE[1]

$As^{3+} + 3\,e^{-} \leftrightarrow\ As(0)$, E^0=-0.68 V vs SHE [2]

$As(s) + 3\,H^{+} + 3\,e^{-} \leftrightarrow AsH_3$, E^0=-0.225 V vs SHE

Taking into account our Ag/AgCl reference to be at -0.197 V vs SHE, the temperature (22°C), the concentrations of the species and the pH=13, the electrochemical reduction potentials is:

$$E_{H2} = E_{H2}^{0} - \frac{0.0254\,V}{2} ln \frac{1}{(10^{-13})^{2}} = -0.957\,V \text{ vs Ag/AgCl}$$

$$E_{As} = E_{As}^{0} - \frac{0.0254\,V}{3} ln \frac{1}{(0.78\;10^{-3})} = -0.938\,V \text{ vs Ag/AgCl}$$

$$E_{AsH3} = E_{AsH3}^{0} - \frac{0.0254\,V}{3} ln \frac{1}{(10^{-13})^{3}} = -1.182\,V \text{ vs Ag/AgCl}$$

S3. EDX maps of the surface of samples with different applied biases

Figure S3 shows the EDX maps of the grown InAs samples with different applied biases. Namely, (a) -1.175 V, (b) -1.25 V, (c) -1.3 V, (d) -1.325 V and (e) -1.35 V. These samples were grown for 90 min using a 0.78 mM As(III) solution. In these maps, the presence of As is red highlighted, and the presence of In is blue highlighted. As seen, the As is mainly present in the Islands that are formed after electrodeposition. These islands were not present on the In substrate as seen figure S3f.

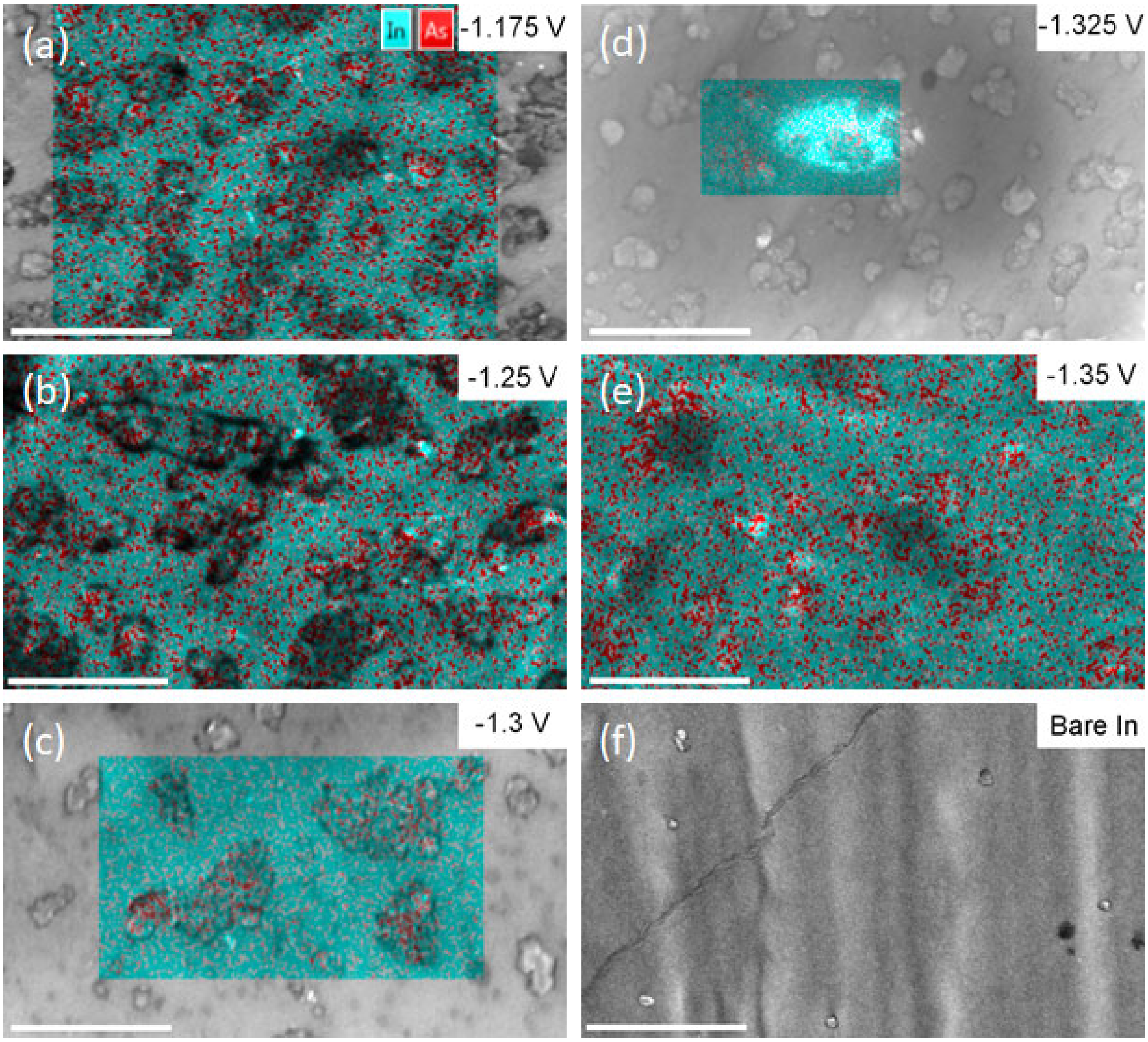

Figure S3. (a-e) EDX maps for samples with different applied biases. The As is highlighted in red, and the In is highlighted in blue. The EDX maps were obtained using a tube voltage of 10 kV, a current of 1.4 nA and a working distance of 5.6 mm. (f) SEM image of a bare In substrate, which was obtained using 5 kV, 100 pA and a working distance of 4.4 mm. Scale bar is 500 nm.

S4. Atomic force microscopy (AFM)

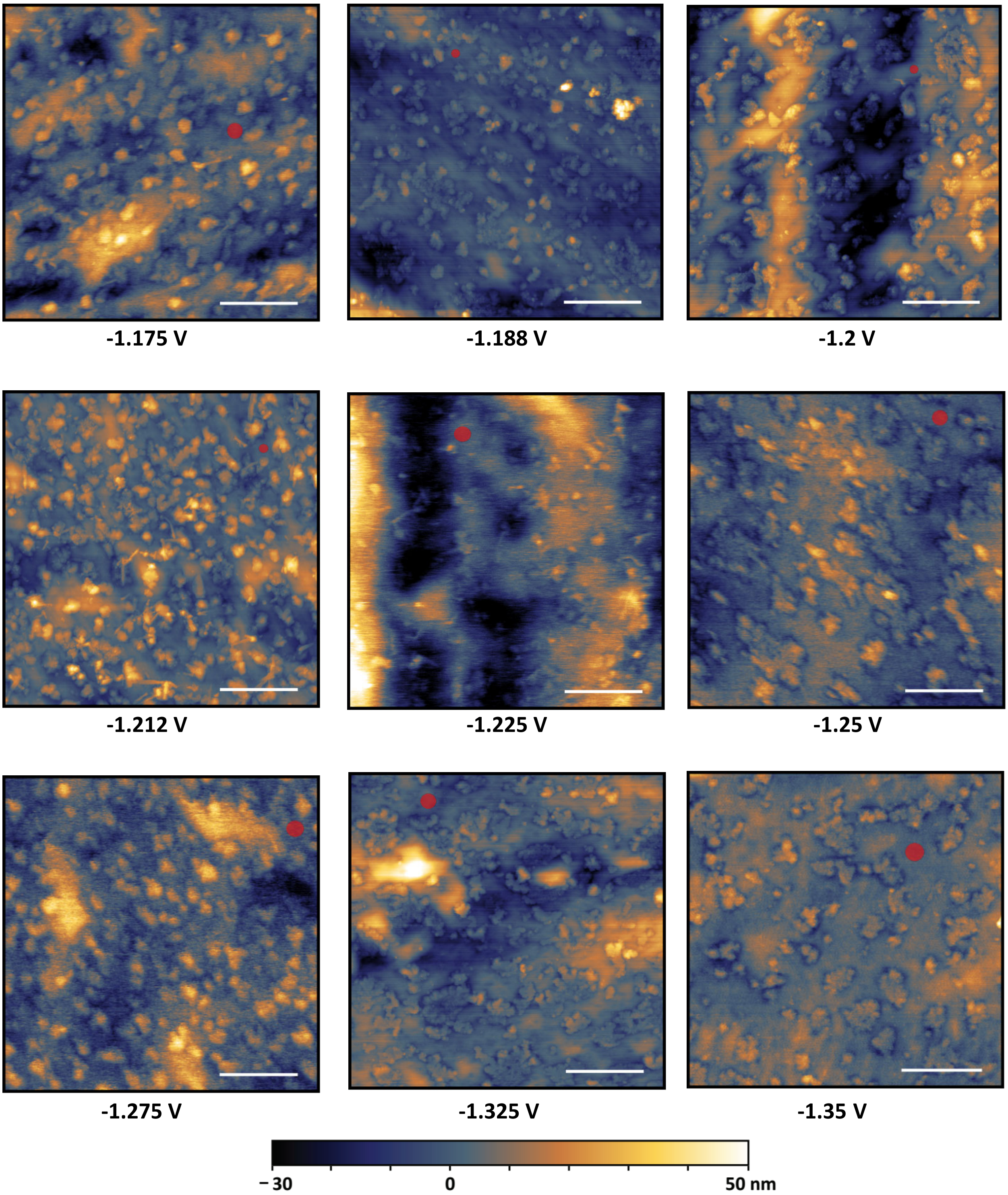
-1.175 V
-1.188 V
-1.2 V
-1.212 V
-1.225 V
-1.25 V
-1.275 V
-1.325 V
-1.35 V

Figure S4-1. AFM topography images (2 μm^2) of the indium foils after As deposition at the potentials as mentioned in the main text. Due to the folds in the underlying foil and the lack of a base plane, 0 height has been defined for every image as indicated by the red dot, so that the colorscale could be kept the same for the purpose of comparison. The scalebar is 500 nm. Reference images are on the next page.

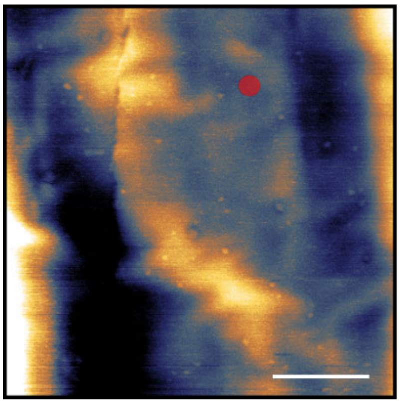

In foil reference

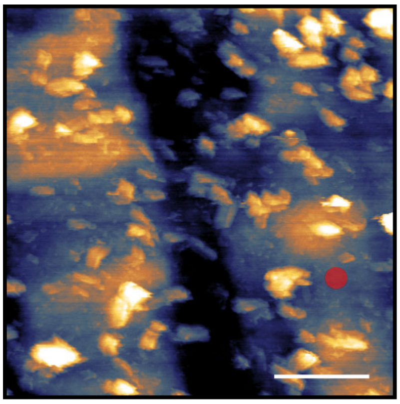

Without As precursor

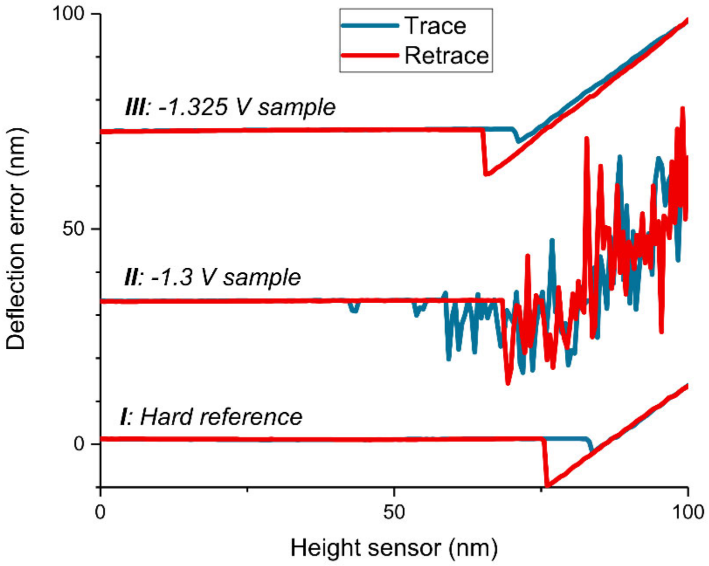

Figure S4-2. Force curves executed sequentially on ***I)*** A hard reference sample, ***II)*** The -1.3 V sample, and ***III)*** The -1.325 V sample as shown in S4-1. The measured cantilever deflection and height value are offset for clarity.

The AFM topography images show protruding nano-islands for all applied potentials, absent on the Indium reference. It should be noted that the image quality on the Indium foils varied from sample to sample for reasons unknown to us (S4-1), but was found to be concurrent with severe noise while executing a force curve (S4-2). As this was an effect of the sample rather than the tip, we were unable to image the -1.3 V sample. All images were obtained with a ScanAsyst-Air probe (r_{nom} = 2 nm, k_{nom} = 0.4 N/m), operated in peakforce tapping mode on a Bruker Dimension Icon AFM. Images were treated by removing the polynomial background (1^{st} order), and aligning rows using the Gwyddion Software [3]. The aligning rows step was done for contrast purposes in the nano-islands, but might remove real features in the underlying indium foil.

S5. Cross section EDX spectrum.

Cross sections of the samples have been made in order to study the thickness of the InAs for various potentials. The cross sections are made using a Ga focused ion beam (FIB) using the FEI Helios Nanolab (30 keV, 9.7 pA). Before milling, a thin layer (500 nm) of Pt was deposited to protect the surface. In order to reduce the EDX signal originating from the Indium substrate, a thin slab of approximately 400 nm was made by milling away both sides as shown in Figure S5-1a. Subsequently an EDX line scan was taken parallel (Figure S5-2a) and perpendicular (Figure S5-2b) to the In-Pt interface as indicated in Figure S5-1b. The white crosses indicate where the reconstructed spectra of Figure S5-2c was obtained. The inset of Figure S5-1b shows the magnified SEM image where one can see an oval shaped dark spot.

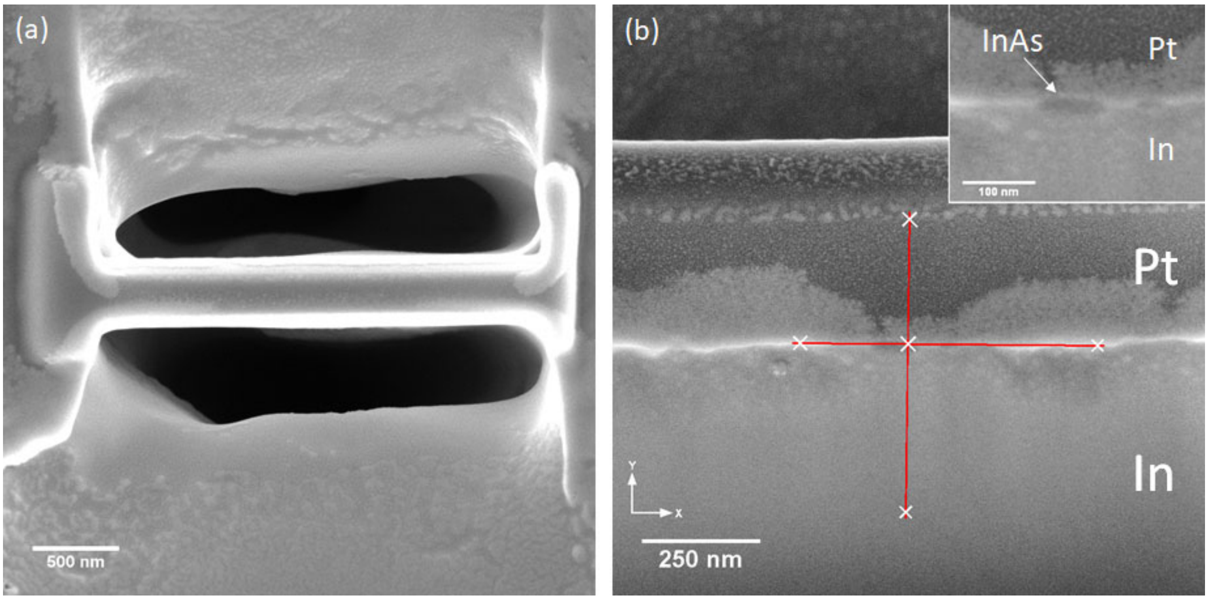

Figure S5-1. SEM images (a) after FIB and (b) indicating where the line scans were obtained. The white crosses represent the position of the reconstructed EDX spectra in Figure S5-2c. The inset shows an magnified area around the centre of the taken line spectra. Both SEM images were taken using 5 kV and 100 pA and using a tilt of (a) 0° and (b) 52°.

The EDX line data shows that this dark spot contains more As than the region outside the spot as can be seen in Figure S5-2a and in the inset of Figure S5-2c. Furthermore, the line scan perpendicular to the interface (Figure S5-2b) also shows that there is no As peak present up until the black spot, indicating that there is no As present below the black spot. Due to the used tilt of 52° while acquiring the EDX line data, there is still a small As peak present above the black spot because the interaction volume of the electrons still include the In-Pt interface. Another result of the used tilt is the gradually increase of the element Pt in the interaction volume of the electron beam. This causes the observed gradually increase of the element Pt and thereby decrease of the element In as shown in figure 2d in the main text and Figure S5-2c. However, as seen in the inset of Figure S5-2c, the reconstructed spectra at the top of the perpendicular scan does not show an As peak. Taking the EDX maps of the surface into account (Figure S5-1), it is most likely that there is no As present at the In-Pt interface deeper into the slab. The presence of Ga is the result of the used Ga focussed ion beam for creating the cross section.

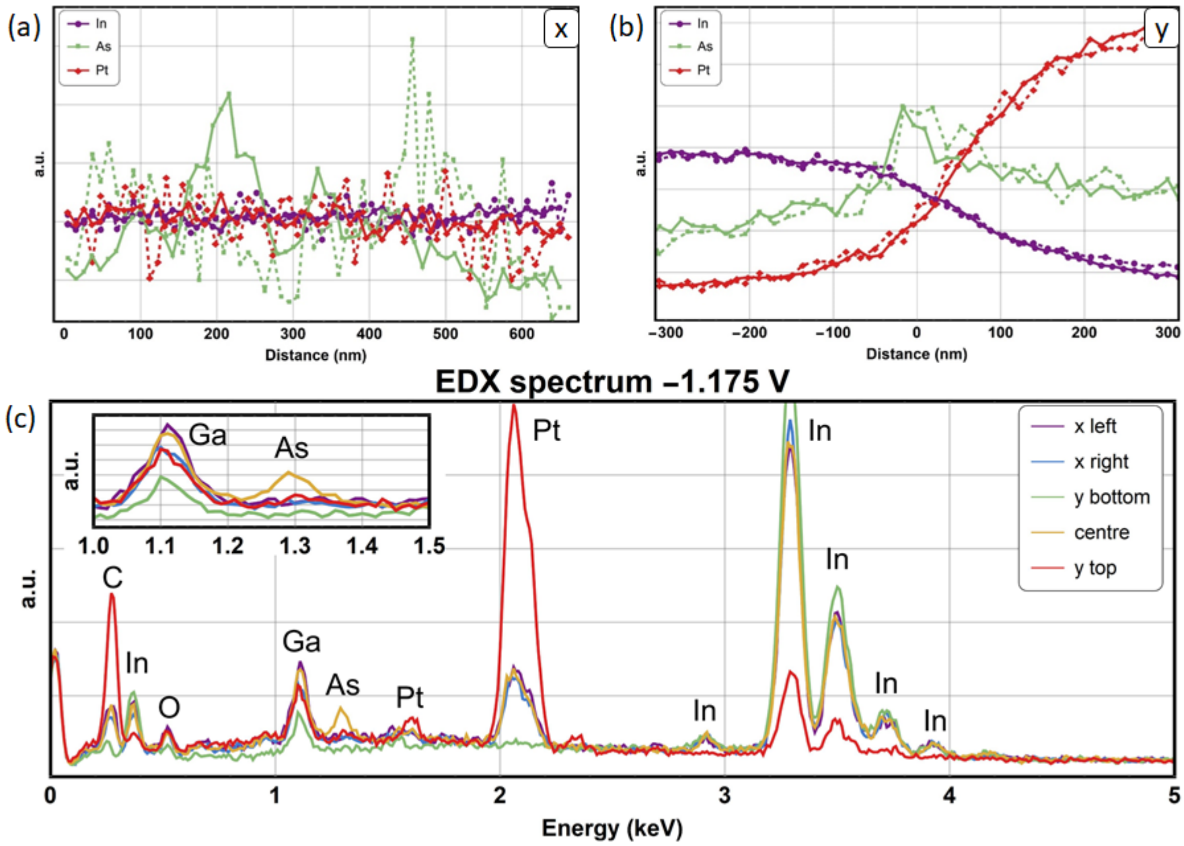

Figure S5-2. EDX line scan for samples at bias -1.175 V (solid) and -1.35 V (dashed) using a tilt of 52° (a) parallel and (b) perpendicular to the interface. The lines of In, As and Pt represent the height of these specific peaks. (c) EDX reconstructed spectra of specific points of the line scan for sample at bias -1.175 V. The inset shows a magnified view of the As peak. Both samples were grown for 90 min in 0.78 mM As(III), 0.1 M NaOH, 0.1 M Na_2SO_4 and 33 mM Cl^-.

S6. Transmission electron microscopy

The lamella was prepared by focused ion beam (FIB). Given the nature of the In metallic substrate, which is prone to extreme amorphization, an exceptionally thick protective platinum double layer was deposited to increase the mechanical stability of the prepared lamella. First, a top layer of platinum was deposited on the sample by e-beam evaporation. A second layer of platinum was deposited locally with a focused ion beam. The poor stability of the sample resulted in sub-prime thinning procedure, and thus a final thickness of the region of interest (i.e. InAs nanocrystal) was too thick for high resolution imaging. All the images and the SAED patterns were acquired in a JEM 2011 LaB_6 (filament) at an acceleration voltage of 200 kV belonging to the *servei de microscòpia (serveis científícotècnics) de la UAB (Universidad Autonoma de Barcelona).*

Figure S6 is a general low resolution TEM image, and the selected area electron diffraction (SAED) patterns of two regions in the lamella, marked by circles. The minimum area selection aperture for the SAED was larger than the islands. Thus, the acquisition of an extra SAED pattern at the substrate allows us to distinguish the reflections related to In, and those arising from the InAs.

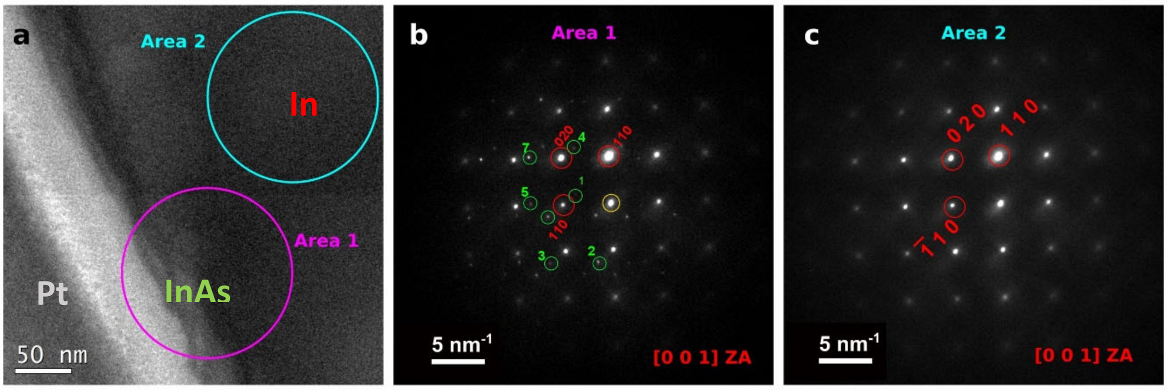

Figure S6. (a) Low resolution TEM image of the cross-section lamella. (b-c) respective SAED obtained in the areas marked in (a) with circles. Area 1 corresponds to a region with both the InAs layer and the In substrate and Area 2 to a region with only substrate.

The spots in green in Figure S6b are the reflections arising from the InAs layer, the ones in red correspond to the substrate. Since the islands are clearly not in zone axis, the analysis of the possible families of planes are carried out comparing the distances measured in Fig. S6b and the theoretical interplanar distances from the InAs reported structures (wurtzite and Zinc blende). The results are listed in table 1.

To summarize, spot 1 can only correspond to zinc-blende InAs. While spots 2-3 agree more closely to distances listed for the zinc-blende structure, spots 4, 5 and 7 agree more to those for the wurtzite one. Finally, The 6th spot is ambiguous.

Spot number	Measured interplanar spacing [A]	Wurtzite spacings [A] / families of planes	Zinc Blende spacings [A] / families of planes
1	3.051	-	3.029 / (200)
2	1.838	1.819 / (-1-12)	1.827 / (-113)
3	1.691	1.631 / (0-22)	1.680 / (0-23)
4	1.593	1.582 / (0-14)	1.515 / (400)
5	1.370	1.366 / (12-1)	1.355 / (402)
6	1.281	1.270 / (0-24)	1.292 / (3-23)
7	1.153	1.159 / (03-2)	1.166 / (3-33)

Table S6 Interplanar distances calculated as the inverse of the measured distances in Fig. S6b and closer theoretical values of interplanar distances for the listed InAs atomic structures with the corresponding families of planes.

S7. Raman spectra

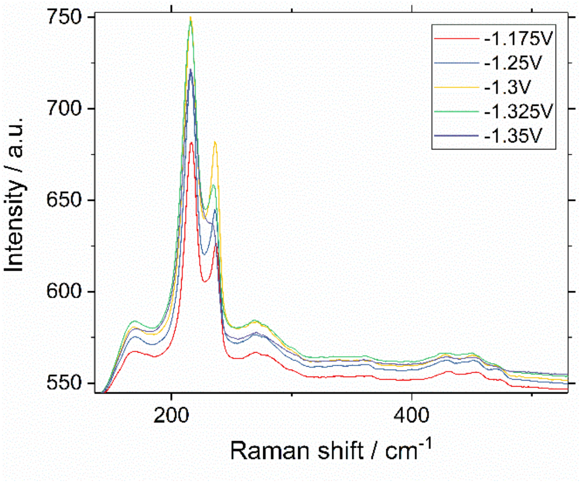

Figure S7-1. Raman spectra showing the first and second order Raman peaks of InAs grown by electrodeposition of As on In foils at different applied cathodic potentials.

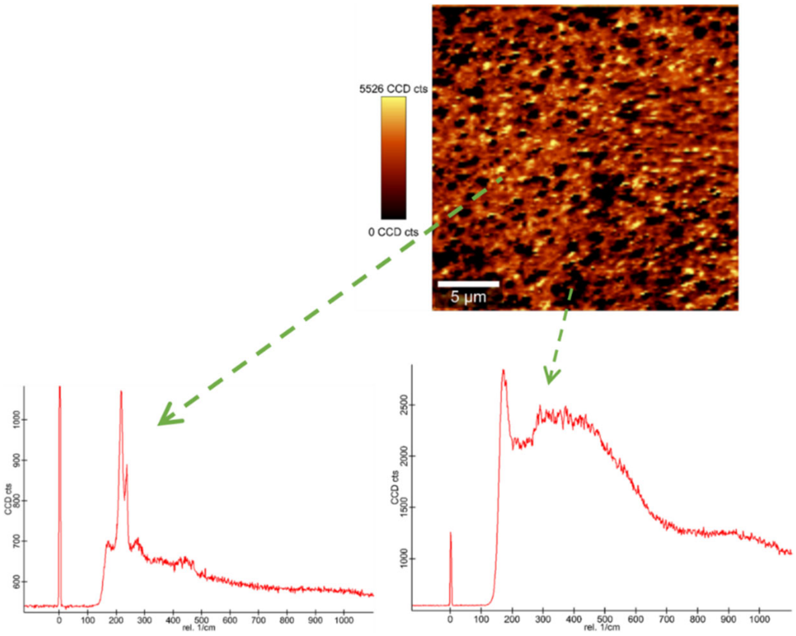

Figure S7-2. Shows a Raman map for the InAs sample grown at -1.35 V vs. Ag/AgCl. The colour of the pixels represents the area under the LO and TO Raman peaks. Characteristic Raman spectra at the bright and dark regions in the map are also shown.

S8. Approximated phonon dispersion of InAs

The theoretical LO peak shift and linewidth shown in Figure 5 was calculated with Eq. 3. The phonon dispersion term (ω (q)) was estimated with the following cosine function that predicts the reported value at the Brillouin zone edge (237.65 cm^{-1} at Γ)[4] and the reported decrease in frequency (39.6 cm^{-1})[5] when going from Γ to X.

$$\omega = 198.05 + 39.6(\cos(\pi q))$$

S9. Calculations of the maximum film thickness of InAs

In order to calculate the maximum thickness of the InAs films from the integrated current, a few assumptions have to be made. The first assumption is that we have a flat In surface with an area of 28.27 mm^2 (diameter 6 mm). The second assumption is that we have 100% Faraday efficiency for As deposition. The third assumption is that the electrodeposited As reacts one to one with the In substrate, without defects and strain. Then we can use the bulk molar mass and density of InAs to calculate the maximum film thickness. The maximum thickness is calculated as follows. First the absolute value of the total charge, Q, is determined by integrating the current over the full 90 min electrodepostion. Then the total electrodeposited moles of As, $N_{As,}$ is calculated by dividing the total charge (Q) by the number of involved electrons, n, and by Faraday's constant, F. Then the maximum thickness, d_{InAs}, is calculated by multiplying N_{As} by the molar mass of InAs, M_{InAs}, and by dividing by the cell area, A_{cell}, and by the density of InAs, ρ_{InAs}.

$$d_{InAs} = \frac{Q}{nF} \frac{M_{InAs}}{A_{cell}\,\rho_{InAs}}$$

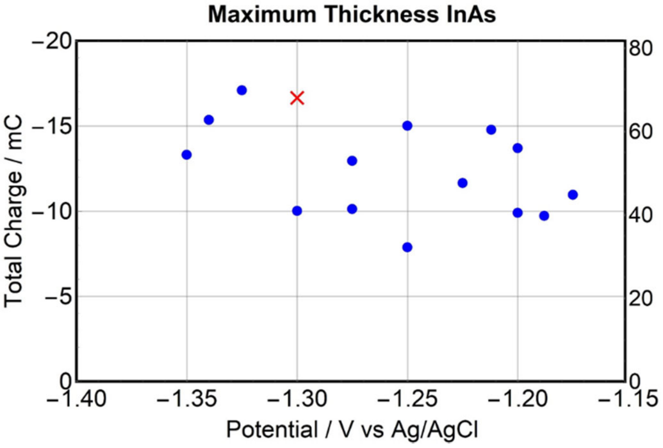

Figure S9. Maximum InAs thickness that can be achieved with the measured total charge during the chronoamperometry (CA) experiments at different applied potentials for electrolytes containing As(III) ions (blue data points). The red cross corresponds to the total charge when the CA is carried out without As(III) precursor in the electrolyte.

S10. Electrochemical cell

The electrochemical cell used in this work has an electrolyte volume capacity of ~ 2ml. The reference microelectrode is placed right in front of the working electrode (blue area in Figure S10). The cell is leak tight and has a gas inlet and outlet to remove any possible arsine gas directly to the exhaust of the fume hood.

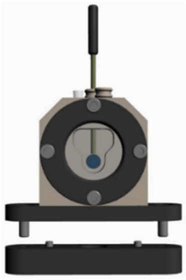

Figure S10. Electrochemical cell.

References

(1) Electrochemical series, Petr Vanýsek

(2) Standard potentials in aqueous solution by Allen j. Bard, Roger Parsons, Joseph Jordan.

(3) D. Necas and P. Klapetek, Cent. Eur. J. Phys., 2012, 10, 181.

(4) Tanta, R.; Lindberg, C.; Lehmann, S.; Bolinsson, J.; Carro-Temboury, M. R.; Dick, K. A.; Vosch, T.; Jespersen, T. S.; Nygård, J. Micro-Raman Spectroscopy for the Detection of Stacking Fault Density in InAs and GaAs Nanowires. *Phys. Rev. B* **2017**, *96* (16), 165433.

(5) Carles, R.; Saint-Cricq, N.; Renucci, J. B.; Renucci, M. A.; Zwick, A. Second-Order Raman Scattering in InAs. *Phys. Rev. B* **1980**, *22* (10), 4804–4815.